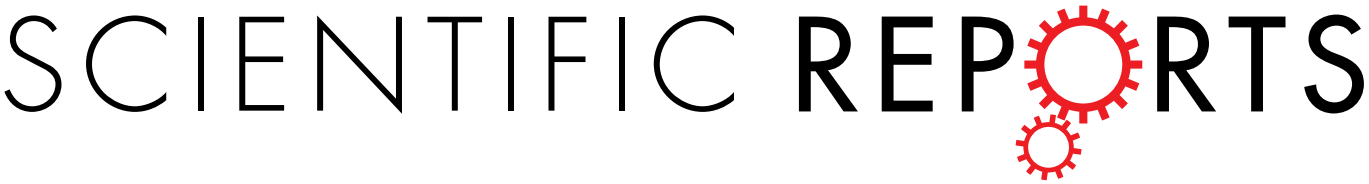

OPEN

Onset of static and dynamic universality among molecular models of polymers

Received: 10 May 2017
Accepted: 12 July 2017
Published online: 28 September 2017

Kazuaki Z. Takahashi[1,2], Ryuto Nishimura[2], Nobuyoshi Yamato[2], Kenji Yasuoka[2] & Yuichi Masubuchi[3]

A quantitatively accurate prediction of properties for entangled polymers is a long-standing challenge that must be addressed to enable efficient development of these materials. The complex nature of polymers is the fundamental origin of this challenge. Specifically, the chemistry, structure, and dynamics at the atomistic scale affect properties at the meso and macro scales. Therefore, quantitative predictions must start from atomistic molecular dynamics (AMD) simulations. Combined use of atomistic and coarse-grained (CG) models is a promising approach to estimate long-timescale behavior of entangled polymers. However, a systematic coarse-graining is still to be done for bridging the gap of length and time scales while retaining atomistic characteristics. Here we examine the gaps among models, using a generic mapping scheme based on power laws that are closely related to universality in polymer structure and dynamics. The scheme reveals the characteristic length and time for the onset of universality between the vastly different scales of an atomistic model of polyethylene and the bead-spring Kremer–Grest (KG) model. The mapping between CG model of polystyrene and the KG model demonstrates the fast onset of universality, and polymer dynamics up to the subsecond time scale are observed. Thus, quantitatively traceable timescales of polymer MD simulations can be significantly increased.

Entangled polymers are widely used in many industrial applications. Despite many years of basic polymer research and industrial use, quantitatively accurate predictions of polymer properties is a long-standing problem that is of great importance for efficient improvement of those properties. The complex structures, dynamics, and physical properties of polymers can change dramatically over different time scales[1–3]. However, phenomena occurring over a wide range of timescales are closely related to each other; *i.e.*, parameters at the atomistic scale can affect properties at the meso and macro scales. Therefore, predictions of polymer properties require atomistic molecular dynamics (AMD) simulations.

While recent advances in computation have enabled a wide range of AMD simulations of chemical and biological polymers[4–12], fully atomistic simulations of entangled polymer dynamics over long timescales are beyond the capability of current platforms. Thus, coarse-grained (CG) MD simulations have been used for long timescales. They can accelerate simulations by reducing the number of degrees of freedom and increasing the fundamental time scale. Accessible polymer characteristics depend on the coarse-graining level, which determines the smallest length scale to trace the polymer dynamics. Models with various CG levels have been developed for long timescale behaviors of polymers[13–18], and some of the models have great potential for more widespread use. However, one critical issue remains unresolved: namely, systematically determining the CG level to which polymers can be coarse-grained while still appropriately tracing static and dynamic polymer properties[18–22]. One path to attack this challenge is the direct comparison of polymer properties between atomistic and CG models. All CG models can be quantitatively compared with atomistic models through a generic mapping scheme based on experimentally established universality in the structures and dynamics of polymers having different chemistries[1,2,21,23–29]. Here, we examined the gap of length and time scales among models using the mapping scheme that

[1]Multi-scale Soft-matter Simulation Team, Research Center for Computational Design of Advanced Functional Materials, National Institute of Advanced Industrial Science and Technology (AIST), Central 2, 1-1-1 Umezono, Tsukuba, Ibaraki, 305-8568, Japan. [2]Department of Mechanical Engineering, Keio University, 3-14-1 Hiyoshi, Kohoku-ku, Yokohama, Kanagawa, 223-8522, Japan. [3]National Composite Center, Nagoya University, Furocho, Chikusa, Nagoya, 464-8630, Japan. Correspondence and requests for materials should be addressed to K.Z.T. (email: kazu.takahashi@aist.go.jp)

	AMD (standard error)				KGMD (standard error)			
M conditions	M [g/mol]	$\langle R^2 \rangle$ [nm^2]	τ_R [ps]	D [10^{-3} nm^2/ps]	M [m]	$\langle R^2 \rangle$ [σ^2]	τ_R [τ]	D [$10^{-3}\sigma^2/\tau$]
Smallest	282.5	2.61962 (0.00087)	41.19 (0.22)	4.50 (0.17)	20	29.409 (0.020)	414.8 (4.5)	3.51 (0.26)
$\approx M_e$	703.4	8.5151 (0.0098)	266.2 (2.1)	1.473 (0.060)	50	80.42 (0.19)	3108 (49)	0.967 (0.078)
M_c	983.9	12.515 (0.021)	552.1 (5.2)	0.914 (0.039)	70	114.72 (0.39)	6910 (130)	0.640 (0.055)

Table 1. Representative parameters for estimation of scaling factors.

assumed universality for three properties closely related to polymer dynamics that have been described in the Rouse theory[30]. These are the mean square end-to-end distance, the end-to-end relaxation time, and the diffusion coefficient. The gaps were estimated by mapping between the atomistic model of polyethylene (PE) and the bead-spring Kremer–Grest (KG) model[14,17], a linkage between the vastly different scales of AMD and high-level CGMD. The gaps were also estimated by mapping between the multiscale molecular model of polystyrene (PS)[31] and the KG model, which involves linkage among the three different scales AMD, middle-level CGMD, and high-level CGMD. PE and PS are common commercial polymers that have been extensively studied experimentally and theoretically, and several reliable molecular models are currently available. The KG model is the simplest very high-level CG model; it has been widely used for decades. With the exception of plain molecular geometries and excluded volume effects, chemical details are entirely omitted in the KG model. Despite its simplicity, it is highly useful and has been used in a wide range of studies on polymer nanocomposites[32,33], polymer welding[34], polymer brushes[35–37], poly-electrolyte gels[38], thermoresponsive polymers[39], ring polymers[40], polymer collapse[41], healing of polymer interfaces[42,43], and biopolymeric motions[44]. With using the generic mapping scheme, the spatial and temporal gaps among molecular models are systematically and accurately estimated. The gaps provide useful information for determination of appropriate CG level, showing a significant advance that will enable a quantitative solution for the challenging problems described above.

Methodology

For quantitative comparison among polymer models, the length and time scales of CG models should be rescaled by a generic way. Because of the Gaussian nature of long polymers, the length unit is usually arbitrary when the linkage to atomistic models is attempted for the static properties of the global polymer structure. Therefore, we assume universality for the onset of entanglement. The onset specifies the characteristic molecular weight at which the power law exponents describing the relationships between dynamical parameters and the molecular weight change significantly. If this universality is assumed, the length units of two different polymer models can be linked to each other. Once the length unit is fixed, the unit of time can be determined. In CG models, it is determined by comparing dynamical measurements with those obtained by the corresponding atomistic model. For example, the mean square displacement (MSD) of chain centers has been used[22,31,45–51], based on reptation theory that predicts the inflection point in MSD at the characteristic time of entanglement. This strategy is useful because the characteristic time of entanglement does not depend on the molecular weight. Despite the successful use of the linkage strategy, the universality of static and dynamic polymer properties is not fully attained for molecular models used in polymer simulations. Gaussian statistics assumed in Rouse models are not observed in atomistic models unless the molecular weight is sufficiently high. The non-Gaussian nature affects the dynamics, which deviate from predictions of the Rouse model. While these deviations are often concealed in the power law expressions[52,53], this issue should be carefully considered when linking different models.

To obtain a reasonable linkage between the atomistic and CG models, we performed the following four steps. (i) The power law relations between the molecular weight M and the mean square end-to-end distance $\langle R^2 \rangle$, the end-to-end relaxation time τ_R, and the diffusion coefficient D, were evaluated for the atomistic and CG models (see Supplement Material for the simulation conditions). (ii) To determine the mass scaling factor, the critical molecular weight M_c was estimated from the change in $\tau_R - M$ and $D - M$ power law exponents that indicate the onset of entanglement. The entanglement molecular weight, M_e, was also estimated by primitive pass analysis (PPA)[54,55] (see Supplement Material for the results of PPA). (iii) The spatial and temporal scaling factors were calculated using a set of $\langle R^2 \rangle$, τ_R, and D for each M, under the conditions of $M \leq M_c$. (iv) The validity of the scaling factors was evaluated by comparison of $\langle R^2 \rangle$–M, τ_R–M, and $D - M$ power law relations obtained from AMD with those obtained from CGMD, and rescaled by the mass, length, and time scaling factors. Based on these results, a simple and reasonable mapping scheme was evaluated.

Results and Discussion

Evaluation of mapping scheme. Table 1 lists the representative parameters used for the estimation of scaling factors. The variables m, σ, and τ are the units of mass, length, and time for KGMD, respectively. The mass scaling factor can be accurately determined from the M_e or M_C results (for more details of the M_e or M_C values, see Supplement Material for the results of PPA). The spatial and temporal scaling factors can be determined by using any two of the following property combinations: $\langle R^2 \rangle_{AMD}/\langle R^2 \rangle_{KGMD}$, $\tau_{R,AMD}/\tau_{R,KGMD}$, and D_{AMD}/D_{KGMD} (suffixes "AMD" and "KGMD" denote the type of simulation). Therefore, three sets of two factors can be obtained from each condition of M. For the spatial scaling factor, the largest differences between the sets were 19%, 11%, and 2.2% for the smallest M, M_e, and M_c values, respectively. For the temporal scaling factor, the largest differences between the sets were 43%, 23%, and 4.5% for the smallest M, M_e, and M_c values, respectively. Thus, the scaling factors converge at $M = M_c$, irrespective of the particular combination of these three properties. The results also imply that the AMD and KGMD simulations will be in quantitative agreement for the three power

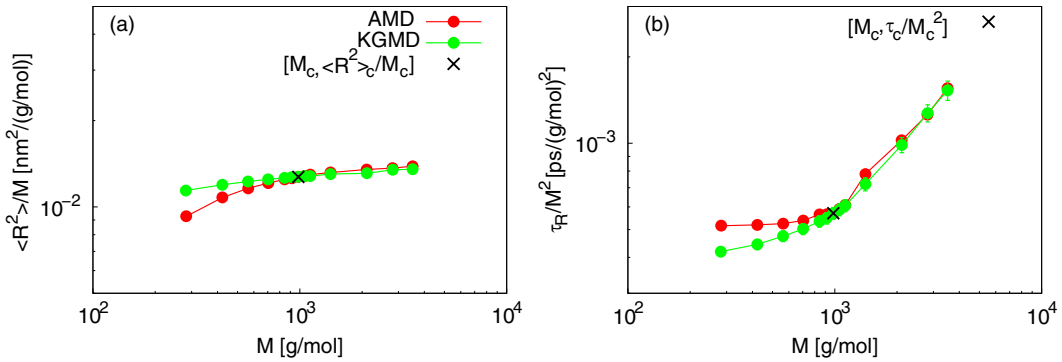

Figure 1. Comparison of power laws between AMD of PE and rescaled KGMD. (**a**) $\langle R^2 \rangle - M$ power law. (**b**) $\tau_R - M$ power law.

laws mentioned above. Therefore, the following equations can be used for estimating the spatial and temporal scaling factors,

$$1\sigma = (\langle R^2 \rangle_{c,AMD} / \langle R^2 \rangle_{c,KGMD})^{1/2} [\mathrm{n}m], \tag{1}$$

$$1\tau = \tau_{c,AMD} / \tau_{c,KGMD} [\mathrm{ps}], \tag{2}$$

where $\langle R^2 \rangle_c$ and τ_c are $\langle R^2 \rangle$ and τ_R at $M = M_c$, respectively. Note that Eqs (1) and (2) are avaliable for any two different MD simulations. From Table 1, it is clear that D_{AMD}/D_{KGMD} should not be used to estimate the scaling factors because the standard errors or deviations were higher for D than for $\langle R^2 \rangle$ and τ_R.

The above scaling factors should be evaluated by comparing $\langle R^2 \rangle - M$, $\tau_R - M$, and $D - M$ power laws from AMD simulations with those obtained from the rescaled KGMD data. Figure 1(a) plots the $\langle R^2 \rangle - M$ power law. The rescaled KGMD results begin to coincide with those from AMD at $M = M_e$, and are almost equal to the AMD values at $M \geq M_c$. This indicates that the spatial scaling factor is reasonable. In contrast, a discrepancy between AMD and KGMD is observed at $M < M_e$. This implies that the spatial scaling factors calculated at $M < M_e$ are inadequate for quantitative static mapping. Figure 1(b) plots the $\tau_R - M$ power law. Similar to the $\langle R^2 \rangle$ results, those from rescaled KGMD start to coincide with the AMD data at $M = M_e$ and are almost identical to AMD values at $M \geq M_c$. This indicates that the temporal scaling factor is reasonable. In contrast, a disagreement between AMD and KGMD was seen at $M < M_e$. This implies that the temporal scaling factors calculated at $M < M_e$ are inadequate for quantitative dynamic mapping. For the $D - M$ power law, the rescaled KGMD results are almost identical to the AMD data (see Fig. S1). Despite the discrepancies between the two types of simulations at $M < M_e$ for $\langle R^2 \rangle$ and τ_R (even at $M < M_e$), the results of KGMD were close to the AMD results. This implies that the use of D may not lead to an accurate estimation of the scaling factors.

These results suggest a simple and reasonable mapping scheme consisting of three steps. (i) Estimate M_c for atomistic and CG models from $\tau_R - M$ (and $D - M$) power law. (ii) Determine the spatial and temporal scaling factors using Eqs (1) and (2). (iii) Evaluate the accuracy of the factors by comparing the $\langle R^2 \rangle - M$, $\tau_R - M$, and $D - M$ power laws obtained from AMD with those obtained from rescaled CGMD. Note that the accuracy of the above scheme relies on the accuracy of the power laws. The uncertainty of power laws reported in previous studies[56–58] implies that a lot of data for long-time trajectories are required for the accurate estimation of the laws. Therefore we carried out long-time MD simulations of atomistic PE (up to 1 microseconds) and bead-spring KG (up to 1 billion time steps) models for a number of initial structures (see Supplement Material for the simulation conditions).

Mapping between atomistic PE and KG models. With using the present mapping scheme, the spacial and temporal gaps of representative static and dynamic properties can be accurately estimated. Figure 2(a) plots the static structure factor, ($S(q)$, for $M \geq M_e$, where q is a spatial frequency that is equal to $2\pi/r$ (r is an intra- or intermolecular distance). The rescaled KGMD results begin to coincide with the AMD data at a threshold value $q_t = 1.78\,rad/nm$, indicating that the onset of static universality between AMD and KGMD occurs at a threshold length $r_t = 3.5\,\mathrm{n}m$, which is equal to the square root of $\langle R^2 \rangle_c$. This implies that the onset of static universality is closely related to M_c. Note that the two simulations can be reasonably linked, even though a true plateau is not reached at the highest M of the present study. Figure 2(b) plots the power law relation between M and the radius of gyration, $\langle R_G^2 \rangle$. The rescaled KGMD results begin to coincide with the AMD values at $M = M_c$. In contrast, the discrepancy between AMD and KGMD is observed at $M < M_c$ because the onset of static universality occurs at $M = M_c$, in agreement with the $S(q)$ results. The results for the radial distribution function, $g(r)$ (see Fig. S2), are consistent with those discussed above. Thus, we have demonstrated that our mapping scheme reveals the characteristic length for the onset of universality between the vastly different scales of AMD and KGMD, for the four static properties $\langle R^2 \rangle$, $\langle R_G^2 \rangle$, $S(q)$, and $g(r)$. The spatial gap between AMD and KGMD is considerably large, raising the discrepancy at $M < M_c$.

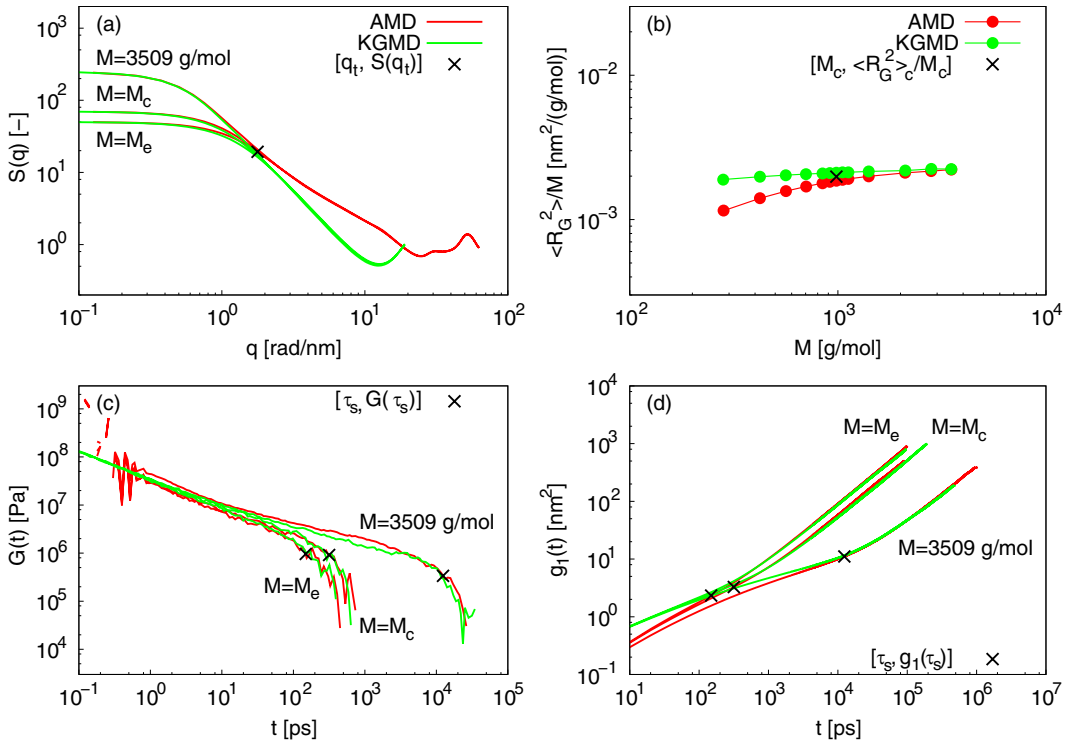

Figure 2. Results of mapping between AMD of PE and KGMD. (**a**) Static structure factors for $M \geq M_e$. (**b**) $\langle R_G^2 \rangle - M$ power law. (**c**) Relaxation modulus for $M \geq M_e$. Also plotted are $[\tau_s, G(\tau_s)]$, where τ_s, is a time at which a shoulder of $G(t)$ occurs. (**d**) MSD of central monomers for $M \geq M_e$. Also plotted are $[\tau_s, g_1(\tau_s)]$, that correspond to the time at which the shoulder of $G(t)$ occurs.

Figure 2(c) plots the relaxation modulus, $G(t)$, for $M \geq M_e$, where t is time. We also plotted $[\tau_s, G(\tau_s)]$, where τ_s is the time when the shoulder of $G(t)$ occurs. For $M = M_e$, M_c, and 3509 g/mol, and $\tau_s = 149$, 316, and 12400 ps, respectively. It was confirmed that τ_s is roughly proportional to τ_R and the terminal relaxation time τ_d (see Fig. S3). The rescaled KGMD results coincide with the AMD values at $t \geq \tau_s$. The coincidence of the AMD and KGMD results at $t < \tau_s$ is partially observed. Figure 2(d) plots the MSD of central monomers, $g_1(t)$, for $M \geq M_e$. Also plotted are $[\tau_s, g_1(\tau_s)]$, for times corresponding to the shoulder of $G(t)$. The rescaled KGMD results coincide with AMD values at $t \geq \tau_s$, in contrast to the large discrepancy between AMD and KGMD data at $t < \tau_s$. This indicates that the onset of dynamic universality for AMD and KGMD occurs at $t = \tau_s$, and that a delay occurs in the onset of dynamic universality depending on M, because τ_s (which is roughly proportional to τ_R and τ_d) increases exponentially with increasing M. This delay arises from differences in chemical structure between the two simulation methods. In KGMD, the chemical details are absent, whereas in AMD, they are included explicitly. This leads to differences in the details of the modeled entanglement. Effects of these differences completely disappear at $t \geq \tau_s$. For the large M (=3509 g/mol), the coincidence of the AMD and KGMD results at $t < \tau_s$ is partially observed. This indicate that the delay in the onset of dynamic universality has a tendency to saturate with increasing M. The results of the autocorrelation function for the end-to-end vector $C(t)$ were consistent with those for τ_R (see Fig. S4). Thus, the mapping scheme reveals the characteristic time for the onset of universality between the vastly different scales of AMD and KGMD, for the five dynamic properties τ_R, D, $C(t)$, $G(t)$, and $g_1(t)$. The temporal gap between AMD and KGMD is considerably large, raising the discrepancy at $t < \tau_s$.

Mapping between multiscale PS and KG models. Harmandaris *et al.* performed multiscale MD (MSMD) simulations of PS melts[31]. The simulations were a combination of AMD and middle-level CGMD that are linked with a specialized mapping scheme. Data for $\langle R^2 \rangle$, $\langle R_G^2 \rangle$, D, and $g_1(t)$ indicate that the rescaled CGMD provides quantitatively accurate results when compared to AMD and experimental data. Here, our mapping scheme was applied to estimate the gap between MSMD data (middle-level CGMD data rescaled by AMD data of PS) and that of KGMD. From the $D - M$ power law of MSMD, $M_{c,MSMD} = 25000$ g/mol and $\langle R^2 \rangle_{c,MSMD} = 82.0\,\mathrm{nm}^2$ (the suffix "MSMD" denotes MSMD simulation). The value $\tau_{c,MSMD} = 2.59 \times 10^8$ ps is estimated from the convergence of the scaling factors discussed above: $\tau_{c,MSMD}/\tau_{c,KGMD} = (\langle R^2 \rangle_{c,MSMD}/\langle R^2 \rangle_{c,KGMD})(D_{c,MSMD}/D_{c,KGMD})^{-1}$. The spatial and temporal scaling factors for this mapping were determined from the above values, KGMD values, and Eqs (1) and (2). Figure 3(a) and (b) plot the $\langle R^2 \rangle - M$ and $D - M$ power laws, respectively. The rescaled KGMD results are almost identical to the MSMD data, confirming the validity of the spatial and temporal scaling factors. Figure 3(c) plots the $\langle R_G^2 \rangle - M$ power law. The rescaled KGMD results are almost equal to those of MSMD, which indicates that the static mapping is reasonable. There was no discrepancy between two models, unlike the mapping between AMD and KGMD. Thus, the spatial gap between the middle-level CG and the KG model is smaller than that between the atomistic and KG models. Figure 3(d) plots the MSD of central monomers at $M = 50000$ g/

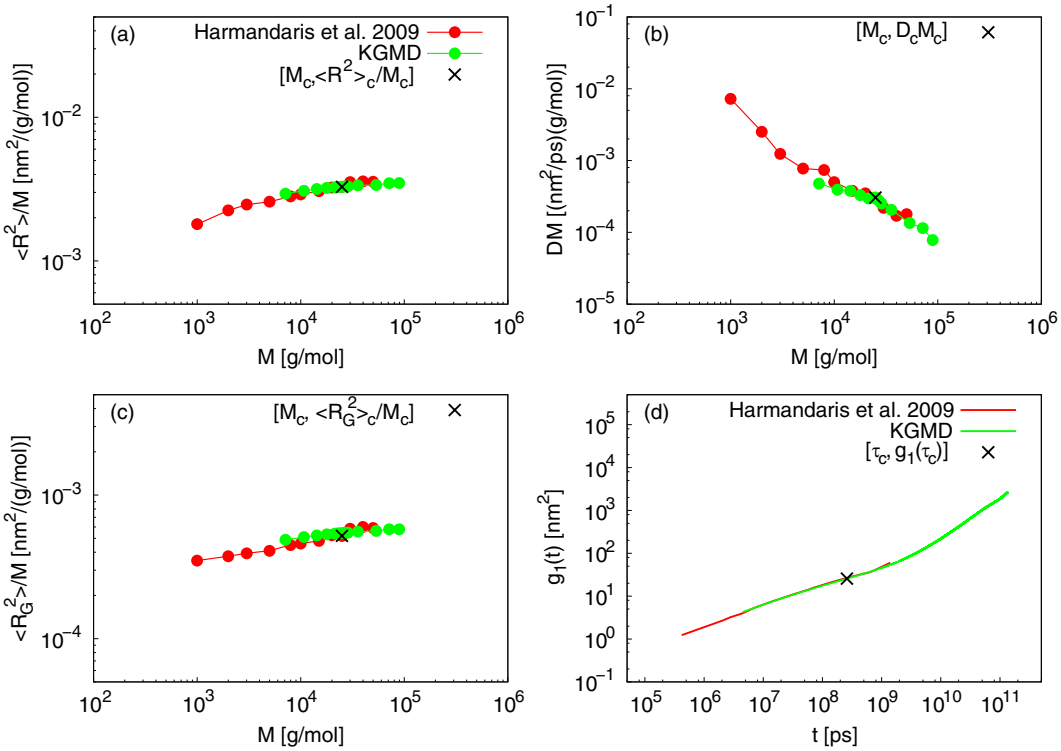

Figure 3. Results of mapping between MSMD of PS and KGMD. (**a**) $\langle R^2 \rangle - M$ power law. (**b**) $D - M$ power law. (**c**) $\langle R_G^2 \rangle - M$ power law. (**d**) MSD of central monomers at $M = 50000$ g/mol.

mol. The interaction points per chain of atomistic, CG, and KG models are 7680 atoms (or 3840 united atoms), 960 particles, and 140 beads, respectively. This implies the efficient multiscale mapping among the three molecular models. The rescaled KGMD results are almost equal to those of MSMD, which indicates that the dynamic mapping is reasonable. Furthermore, the results for $g_1(t)$ are a quantitative estimation of polymer dynamics up to a subsecond time scale (0.135 sec). This highlights the great potential of multiscale mapping for polymer molecular dynamics with realistic time scales. A direct comparison between MD results and experimental data becomes much easier for polymer dynamics, and enables high-throughput screening in polymer development. There was no discrepancy between two models, unlike the mapping between AMD and KGMD. The onset of universality in $g_1(t)$ is much *faster* ($t \ll \tau_c$) than that for mapping between AMD and KGMD. Thus, the temporal gap between the middle-level CG and the KG model is smaller than that between the atomistic and KG models.

Again we focus on the characteristic of the spatial and temporal gaps. The large gaps are observed between AMD and KGMD despite the number of united-atoms per PE chain is almost equal to that of beads per KG chain. In contrast, The gaps between middle-level CGMD and KGMD is small despite the number of CG particles per PS chain is about 7 times larger than that of beads per KG chain. This means that the difference of chemical details (e.g., intra- and intermolecular interactions) is more effective for the gaps than the difference of the plain geometries of polymer models. Significantly, the gaps become small when linking molecular models having not less than a certain CG level. Estimating this level is critical for the development of CG models, because it provides the threshold for the effective coarse-graining achieving a good balance between model accuracy and computational cost. Here the present mapping scheme can reasonably determine the spatial and temporal gaps for representative polymer properties. The quantified gaps are useful as the index for searching the appropriate CG level. Therefore, optimization techniques of coarse-graining for polymer molecular models will be systematically extended by using the present scheme.

Conclusions

The application of universal polymer behavior to the linkage among molecular models at various length and time scales was examined in terms of a mapping scheme focused on power laws that also show universality. The spatial and temporal gaps were evaluated by mapping between the atomistic model of PE and the coarse-grained KG model, a linkage between the vastly different scales of AMD and high-level CGMD. The scheme reveals the characteristic length and time for the onset of universality between AMD and KGMD for the representative static and dynamic properties. The large gaps raise the discrepancies of the properties at short length and time scales, showing the clear limit for bridging the two simulations while retaining atomistic characteristics. To overcome this limit, low-level (*i.e.*, elaborate) CG models that introduce the effects of short length and time scales should be developed[18,20,22]. The scheme was then use to evaluate the gaps between the multiscale molecular models of PS and the KG model, which involves a linkage among the three different scales of AMD, middle-level CGMD, and high-level CGMD. The small gaps between middle- and high-level CGMD attain the fast onset of universality

without the discrepancies of the properties at any length and time scales. Furthermore, it allows a linkage between the two models that quantitatively estimates polymer dynamics up to the subsecond timescale. This demonstrates the great potential to that the combination of various scales of molecular models permits multiscale mapping for polymer MD simulations. Here, quantitatively traceable MD time ranges can be significantly scaled up, which introduces the possibility of direct linkage between MD simulations and macroscale approaches[59,60]. The present mapping scheme is simple, and the scaling factors can be estimated with reasonable accuracy by using existing MD simulations and computational resources. Therefore, it is anticipated that it will be applicable to the sequential multiscale mapping among AMD, low-, middle-, and high-level CGMD for quantitative estimation of polymer properties at realistic length and time scales while maintaining a reasonable computational cost.

References

1. Doi, M. & Edwards, S. F. *The theory of polymer dynamics*, volume 73. oxford university press (1988).
2. Ferry, J. D. *Viscoelastic properties of polymers*. John Wiley & Sons (1980).
3. Masubuchi, Y. Simulating the flow of entangled polymers. *Annual review of chemical and biomolecular engineering* **5**, 11–33 (2014).
4. Baig, C., Mavrantzas, V. G. & Kr'oger, M. Flow effects on melt structure and entanglement network of linear polymers: Results from a nonequilibrium molecular dynamics simulation study of a polyethylene melt in steady shear. *Macromolecules* **43**(16), 6886–6902 (2010).
5. Barrat, J.-L., Baschnagel, J. & Lyulin, A. Molecular dynamics simulations of glassy polymers. *Soft Matter* **6**(15), 3430–3446 (2010).
6. Chung, H. S., Piana-Agostinetti, S., Shaw, D. E. & Eaton, W. A. Structural origin of slow diffusion in protein folding. *Science* **349**(6255), 1504–1510 (2015).
7. Do, C. *et al*. Li+ transport in poly (ethylene oxide) based electrolytes: neutron scattering, dielectric spectroscopy, and molecular dynamics simulations. *Physical review letters* **111**(1), 018301 (2013).
8. Hossain, D. *et al*. Molecular dynamics simulations of deformation mechanisms of amorphous polyethylene. *Polymer* **51**(25), 6071–6083 (2010).
9. Hur, K. *et al*. Chain dynamics of ring and linear polyethylene melts from molecular dynamics simulations. *Macromolecules* **44**(7), 2311–2315 (2011).
10. Mitchell, J. S. & Harris, S. A. Thermodynamics of writhe in dna minicircles from molecular dynamics simulations. *Physical review letters* **110**(14), 148105 (2013).
11. Ndoro, T. V. *et al*. Interface of grafted and ungrafted silica nanoparticles with a polystyrene matrix: Atomistic molecular dynamics simulations. *Macromolecules* **44**(7), 2316–2327 (2011).
12. Stephanou, P. S., Baig, C., Tsolou, G., Mavrantzas, V. G. & Kröger, M. Quantifying chain reptation in entangled polymer melts: Topological and dynamical mapping of atomistic simulation results onto the tube model. *The Journal of chemical physics* **132**(12), 124904 (2010).
13. Brini, E. *et al*. Systematic coarse-graining methods for soft matter simulations–a review. *Soft Matter* **9**(7), 2108–2119 (2013).
14. Everaers, R. *et al*. Rheology and microscopic topology of entangled polymeric liquids. *Science* **303**(5659), 823–826 (2004).
15. Groot, R. D. & Warren, P. B. Dissipative particle dynamics: Bridging the gap between atomistic and mesoscopic simulation. *Journal of Chemical Physics* **107**(11), 4423 (1997).
16. Jury, S. *et al*. Simulation of amphiphilic mesophases using dissipative particle dynamics. *Phys. Chem. Chem. Phys.* **1**(9), 2051–2056 (1999).
17. Kremer, K. & Grest, G. S. Dynamics of entangled linear polymer melts: A molecular-dynamics simulation. *The Journal of Chemical Physics* **92**, 5057 (1990).
18. McCarty, J., Clark, A., Copperman, J. & Guenza, M. An analytical coarse-graining method which preserves the free energy, structural correlations, and thermodynamic state of polymer melts from the atomistic to the mesoscale. *The Journal of chemical physics* **140**(20), 204913 (2014).
19. Karimi-Varzaneh, H. A., van der Vegt, N. F., Müller-Plathe, F. & Carbone, P. How good are coarse-grained polymer models? a comparison for atactic polystyrene. *Chem Phys Chem* **13**(15), 3428–3439 (2012).
20. Liu, L., Padding, J., Den Otter, W. & Briels, W. Coarse-grained simulations of moderately entangled star polyethylene melts. *The Journal of chemical physics* **138**(24), 244912 (2013).
21. Pérez-Aparicio, R., Colmenero, J., Alvarez, F., Padding, J. & Briels, W. Chain dynamics of poly (ethylene-alt-propylene) melts by means of coarse-grained simulations based on atomistic molecular dynamics. *The Journal of chemical physics* **132**(2), 024904 (2010).
22. Salerno, K. M., Agrawal, A., Perahia, D. & Grest, G. S. Resolving dynamic properties of polymers through coarse-grained computational studies. *Physical review letters* **116**(5), 058302 (2016).
23. Clark, A. & Guenza, M. Mapping of polymer melts onto liquids of soft-colloidal chains. *The Journal of chemical physics* **132**(4), 044902 (2010).
24. Fritz, D., Koschke, K., Harmandaris, V. A., van der Vegt, N. F. & Kremer, K. Multiscale modeling of soft matter: scaling of dynamics. *Physical Chemistry Chemical Physics* **13**(22), 10412–10420 (2011).
25. Lyubimov, I. & Guenza, M. First-principle approach to rescale the dynamics of simulated coarse-grained macromolecular liquids. *Physical Review E* **84**(3), 031801 (2011).
26. Lyubimov, I., McCarty, J., Clark, A. & Guenza, M. Analytical rescaling of polymer dynamics from mesoscale simulations. *The Journal of chemical physics* **132**(22), 224903 (2010).
27. Padding, J. & Briels, W. Systematic coarse-graining of the dynamics of entangled polymer melts: the road from chemistry to rheology. *Journal of Physics: Condensed Matter* **23**(23), 233101 (2011).
28. Peter, C. & Kremer, K. Multiscale simulation of soft matter systems–from the atomistic to the coarse-grained level and back. *Soft Matter* **5**(22), 4357–4366 (2009).
29. Peter, C. & Kremer, K. Multiscale simulation of soft matter systems. *Faraday discussions* **144**, 9–24 (2010).
30. Rouse, P. E. Jr. A theory of the linear viscoelastic properties of dilute solutions of coiling polymers. *The Journal of Chemical Physics* **21**(7), 1272–1280 (1953).
31. Harmandaris, V. A. & Kremer, K. Dynamics of polystyrene melts through hierarchical multiscale simulations. *Macromolecules* **42**(3), 791–802 (2009).
32. Feng, Y. *et al*. Role of block copolymer morphology on particle percolation of polymer nanocomposites. *Soft matter* **10**(41), 8236–8244 (2014).
33. Wang, Z., Liu, J., Wu, S., Wang, W. & Zhang, L. Novel percolation phenomena and mechanism of strengthening elastomers by nanofillers. *Physical Chemistry Chemical Physics* **12**(12), 3014–3030 (2010).
34. Ge, T., Pierce, F., Perahia, D., Grest, G. S. & Robbins, M. O. Molecular dynamics simulations of polymer welding: Strength from interfacial entanglements. *Physical review letters* **110**(9), 098301 (2013).
35. Binder, K., Kreer, T. & Milchev, A. Polymer brushes under flow and in other out-of-equilibrium conditions. *Soft Matter* **7**(16), 7159–7172 (2011).
36. Binder, K. & Milchev, A. Polymer brushes on flat and curved surfaces: How computer simulations can help to test theories and to interpret experiments. *Journal of Polymer Science Part B: Polymer Physics* **50**(22), 1515–1555 (2012).

37. Galuschko, A. *et al*. Frictional forces between strongly compressed, nonentangled polymer brushes: molecular dynamics simulations and scaling theory. *Langmuir* **26**(9), 6418–6429 (2010).
38. Longo, G. S., Olvera de La Cruz, M. & Szleifer, I. Molecular theory of weak polyelectrolyte gels: the role of ph and salt concentration. *Macromolecules* **44**(1), 147–158 (2010).
39. Vagias, A. *et al*. Complex tracer diffusion dynamics in polymer solutions. *Physical review letters* **111**(8), 088301 (2013).
40. Goossen, S. *et al*. Molecular scale dynamics of large ring polymers. *Physical review letters* **113**(16), 168302 (2014).
41. Mukherji, D., Marques, C. M. & Kremer, K. Polymer collapse in miscible good solvents is a generic phenomenon driven by preferential adsorption. *Nature communications* **5** (2014).
42. Ge, T., Robbins, M. O., Perahia, D. & Grest, G. S. Healing of polymer interfaces: Interfacial dynamics, entanglements, and strength. *Physical Review E* **90**(1), 012602 (2014).
43. Stukalin, E. B., Cai, L.-H., Kumar, N. A., Leibler, L. & Rubinstein, M. Self-healing of unentangled polymer networks with reversible bonds. *Macromolecules* **46**(18), 7525–7541 (2013).
44. Brackley, C. A., Taylor, S., Papantonis, A., Cook, P. R. & Marenduzzo, D. Nonspecific bridging-induced attraction drives clustering of dna-binding proteins and genome organization. *Proceedings of the National Academy of Sciences* **110**(38), E3605–E3611 (2013).
45. Chen, C., Depa, P., Maranas, J. K. & Sakai, V. G. Comparison of explicit atom, united atom, and coarse-grained simulations of poly (methyl methacrylate). *The Journal of chemical physics* **128**(12), 124906 (2008).
46. Chen, C. *et al*. A comparison of united atom, explicit atom, and coarse-grained simulation models for poly (ethylene oxide). *The Journal of chemical physics* **124**(23), 234901 (2006).
47. Depa, P. K. & Maranas, J. K. Speed up of dynamic observables in coarse-grained molecular-dynamics simulations of unentangled polymers. *The Journal of chemical physics* **123**(9), 094901 (2005).
48. Depa, P. K. & Maranas, J. K. Dynamic evolution in coarse-grained molecular dynamics simulations of polyethylene melts. *The Journal of chemical physics* **126**(5), 054903–054903 (2007).
49. Harmandaris, V., Adhikari, N., van der Vegt, N. F. & Kremer, K. Hierarchical modeling of polystyrene: From atomistic to coarse-grained simulations. *Macromolecules* **39**(19), 6708–6719 (2006).
50. Harmandaris, V. A., Reith, D., Van der Vegt, N. F. & Kremer, K. Comparison between coarse-graining models for polymer systems: Two mapping schemes for polystyrene. *Macromolecular chemistry and physics* **208**(19–20), 2109–2120 (2007).
51. Leon, S., van der Vegt, N., Delle Site, L. & Kremer, K. Bisphenol a polycarbonate: entanglement analysis from coarse-grained md simulations. *Macromolecules* **38**(19), 8078–8092 (2005).
52. Takahashi, K. Z., Nishimura, R., Yasuoka, K. & Masubuchi, Y. Molecular dynamics simulations for resolving scaling laws of polyethylene melts. *Polymers* **9**(1), 24 (2017).
53. Takahashi, K. Z., Yamato, N., Yasuoka, K. and Masubuchi, Y. Critical test of bead-spring model to resolve the scaling laws of polymer melts: a molecular dynamics study. *Molecular Simulation*. (in press).
54. Hoy, R. S., Foteinopoulou, K. & Kröger, M. Topological analysis of polymeric melts: Chain-length effects and fast-converging estimators for entanglement length. *Physical Review E* **80**(3), 031803 (2009).
55. Kröger, M. Shortest multiple disconnected path for the analysis of entanglements in two-and three-dimensional polymeric systems. *Computer Physics Communications* **168**(3), 209–232 (2005).
56. Harmandaris, V. *et al*. Crossover from the rouse to the entangled polymer melt regime: signals from long, detailed atomistic molecular dynamics simulations, supported by rheological experiments. *Macromolecules* **36**(4), 1376–1387 (2003).
57. Harmandaris, V. A., Mavrantzas, V. G. & Theodorou, D. N. Atomistic molecular dynamics simulation of polydisperse linear polyethylene melts. *Macromolecules* **31**(22), 7934–7943 (1998).
58. Tsolou, G., Mavrantzas, V. G. & Theodorou, D. N. Detailed atomistic molecular dynamics simulation of cis-1, 4-poly (butadiene). *Macromolecules* **38**(4), 1478–1492 (2005).
59. Leitmann, S., Höfling, F. & Franosch, T. Tube concept for entangled stiff fibers predicts their dynamics in space and time. *Physical Review Letters* **117**(9), 097801 (2016).
60. Xi, H.-D., Bodenschatz, E. & Xu, H. Elastic energy flux by flexible polymers in fluid turbulence. *Physical review letters* **111**(2), 024501 (2013).

Acknowledgements

K. Z. T. was partially supported by Japan Society for the Promotion of Science (JSPS) Grants-in-Aid for Scientific Research (KAKENHI) Grant Number 16H06071.

Author Contributions

K.Z.T., K.Y., and Y.M. designed research; K.Z.T., R.N., and N.Y. performed research; and K.Z.T. wrote the paper.

Additional Information

Supplementary information accompanies this paper at doi:10.1038/s41598-017-08501-0

Competing Interests: The authors declare that they have no competing interests.

Publisher's note: Springer Nature remains neutral with regard to jurisdictional claims in published maps and institutional affiliations.